Hydrometallurgy 212 (2022) 105894

Contents lists available at ScienceDirect

Hydrometallurgy

journal homepage: www.elsevier.com/locate/hydromet

Laccase-mediator system for enzymatic degradation of carbonaceous matter in the sequential pretreatment of double refractory gold ore from Syama mine, Mali

Ryotaro Sakai [a], Diego M. Mendoza [a], Kojo T. Konadu [a], Cindy [a], Yuji Aoki [b], Tsuyoshi Hirajima [a,b], Hirofumi Ichinose [c], Keiko Sasaki [a,*]

[a] Department of Earth Resources Engineering, Kyushu University, Motooka 744, Fukuoka 819-0395, Japan
[b] Niihama Research Institute, Sumitomo Metal Mine Co. Ltd., Niihama 792-0002, Japan
[c] Department of Agro-environmental Sciences, Kyushu University, Motooka 744, Fukuoka 819-0395, Japan

ARTICLE INFO

Keywords:
Double refractory gold ore
Laccase-mediator system
Gold recovery
Ferric chloride leaching
Sequential pretreatment
Three-dimensional fluorescence spectra

ABSTRACT

The sequential bio-treatment of refractory carbonaceous gold ore is a promising solution to recover gold effectively by environmentally friendly technology, which includes bio-oxidation of sulfide and biodegradation of carbonaceous matter by lignin-degrading enzymes. There are several drawbacks in enzyme treatment using cell-free spent medium (CFSM), including lignin peroxidase and manganese peroxidase from *Phanerochaete chrysosporium,* in particular the poor stability of enzyme activities. In the present work, laccase-mediator system (LMS) was applied for the degradation of carbonaceous matter in real gold ore to improve the efficiency of gold extraction as well as handling. The LMS was intended to be a great alternative process of CFSM with utilizing purified laccase in the presence of 1-hydroxybenzotriazole as a mediator. The application of LMS provided several advantages including not only greater stability, greater efficiency to degrade carbonaceous matter, better handling, much saving the treatment time, but also wider availability in laccase. In addition, replacing bio-oxidation with ferric chloride leaching as the dissolution path of sulfides facilitated avoiding the formation of jarosite and saving the required time. The gold recovery by cyanidation was improved from 41.5 ± 0.3% for the starting material to 81.3 ± 3.9% ($n = 2$) for the solid residues after the modified sequential pretreatment. This is correspondent to 86.3% of gold recovery for the extractable maximum gold excluding the enclosed gold in acid-insoluble silicates. The improved process involving LMS can be proposed with valuable advantages to fit a sustainable metallurgical technology of gold ores.

1. Introduction

The cyanidation process has been a royal road to extract gold (Au) from gold ores and utilized for over 130 years in industrial mining because of the high efficiency and reaction rate of the formation of Au $(CN)_2^-$ (Anderson, 2016; Bas et al., 2017). Non-refractory gold ores, in which gold can be easily extracted by cyanidation, are currently under fast exhaustion (Norgate and Haque, 2012). So refractory gold ores are gaining attention for processing and gold extraction on an industrial scale. In these refractory ores, gold grains are locked in sulfides, and cyanide may not be able to access for the complexation. Hence, pretreatment is necessary prior to cyanidation to liberate gold grains from sulfides (Qin et al., 2021). Pressure oxidation (Guzman et al., 2018), bio-oxidation (Suzuki, 2001; Wang et al., 2020), and chemical oxidation (Wang et al., 2020) are known as such pretreatments for sulfidic refractory gold ores. Additionally, the adsorption of $Au(CN)_2^-$ onto very fine grains of carbonaceous matter (CM) caused a decrease in gold extraction during cyanidation. This phenomenon is known as "preg-robbing" where the loss of gold recovery range from a low values to more than 50% (Abotsi and Osseo-Asare, 1986; Amanya et al., 2017; Owusu et al., 2021). Preg-robbing is caused by the presence of graphitic/amorphous elemental carbon in CM of the gold ores. The refractory gold ores, which contain both gold locking in sulfides and preg-robbing by CM, are classified as a double refractory gold ores, abbreviated as DRGOs (Nanthakumar et al., 2007).

In recent years, environmentally friendly and effective pretreatments

* Corresponding author.
E-mail address: keikos@mine.kyushu-u.ac.jp (K. Sasaki).

https://doi.org/10.1016/j.hydromet.2022.105894
Received 30 October 2021; Received in revised form 3 May 2022; Accepted 8 May 2022
Available online 13 May 2022

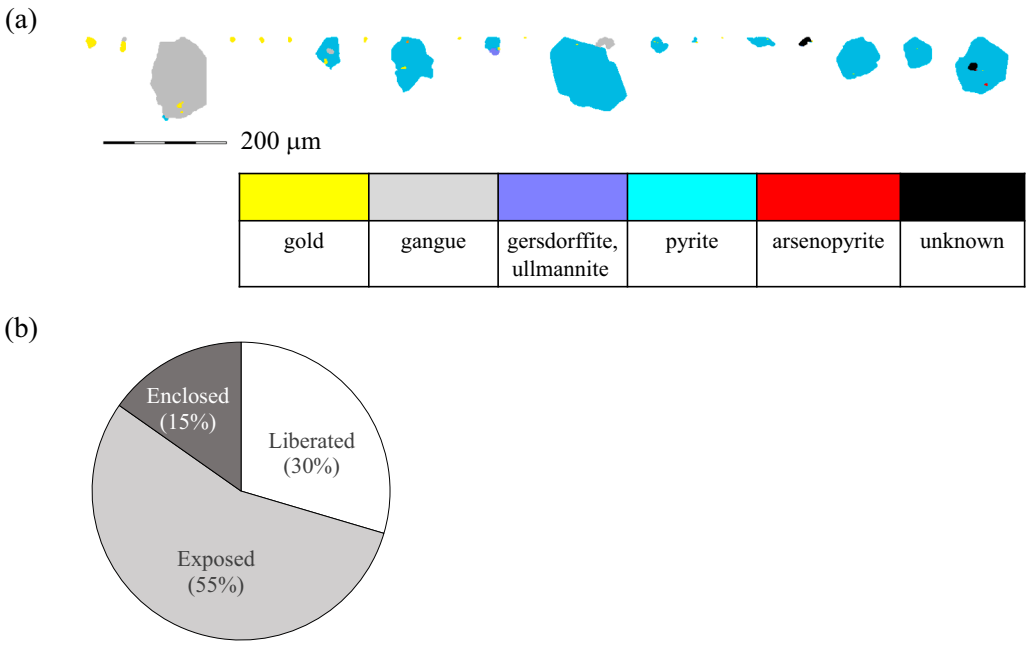

Fig. 1. Mineral liberation analytical results for DRGO from Syama mines, Mali, (a) mineralogical 2D mapping of liberated Au and Au-bearing grains, (b) distributions of liberated, exposed and enclosed Au grains.

for DRGO have been significantly required because of the growing interests of mining industries to recover gold from DRGOs (Konadu et al., 2020). However, degradation of CM appears to be still challenging due to its complicated structures and association with other minerals, low contents but fine particle sizes of carbonaceous matter, and uncertain origin of coalification. Then, biochemical reaction for the degradation of carbonaceous matter has been evaluated to reduce the loss of gold extraction, because of some advantages such as mild conditions, low energy consumption, and eco-friendly nature of bio-processing (Yang et al., 2013). In particular, there have been growing studies of CM degradation by the lignin-degrading enzymes released from *Phanerochaete chrysosporium*, a white-rot fungus, where manganese peroxidase (MnP) and lignin peroxidase (LiP) are included (Konadu et al., 2017; Liu et al., 2016; Ofori-Sarpong et al., 2010; Ofori-Sarpong and Osseo-Asare, 2013).

Recently, it has been proposed a sequential biotreatment of DRGO through two steps including microbiological oxidation of sulfides and enzymatic degradation of CM (Konadu et al., 2019a). In the first step, sulfides were oxidatively decomposed by an iron-oxidizing archaeon for the liberation of gold grains. In the second step, CM was degraded by the enzymatic treatments using cell-free spent medium (CFSM) obtained from *P. chrysosporium*, since the fungal biomass must be eliminated because it might act as an adsorbent for $Au(CN)_2^-$. Followed by alkaline washing, the gold recovery was much improved to 92% from 24% in the original DRGO. Although the above sequential bio-treatment was successfully applied to DRGO, the most serious drawback is inconvenient handling in CFSM treatment caused by poor stabilities of LiP and MnP, resulting in the repetition of the same enzymatic reaction process by replacing the fresh CFSM.

Regarding the enzyme degradation of carbonaceous matter, Mendoza et al. (2021a) reported the degradation characteristics of laccase-mediator system (LMS) using powder-activated carbon. Laccase (Lcc) is also one of the lignin-degrading enzymes, which has several superiorities over CFSM, that is, greater stability, utilization of purified Lcc, wider availability from various species of a white-rot fungus, and applicability of mediator system (Fakoussa and Hofrichter, 1999). As mentioned above, the CFSM does not include Lcc. There are no reports, in which Lcc was applied to degrade carbonaceous matter in DRGO for the metallurgical purpose, to our knowledge. In the present work, LMS was applied to the enzymatic degradation of carbonaceous matter in the sequential treatment of DRGO to improve gold recovery.

2. Material and methods

2.1. Original DRGO, its characterization, and overview of the sequential treatment

The original DRGO was supplied from Syama mines, Mali. The gold content was 24 g/t determined by the fire assay. Mineral liberation analysis (MLA, Thermo, 650 FEG, Waltham, Massachusetts, USA) for the original DRGO revealed that Au types were 30% of the Au liberated grains, 55% of the Au exposed grains, and others enclosed in pyrite (6.6%) and silicates (8.6%) (Fig. 1), indicating the necessity to decompose sulfide, specifically pyrite. The elemental compositions (% *w*/w) based on CHN analysis (Yanaco XMT-5, Kyoto, Japan, Table S1) and X-ray fluorescence (XRF) analysis (Rigaku, ZSX Primus II, Akishima, Japan, Table 1) showed 5.3% C, 13.4% Fe, 15.7% Si and 2.0% K. Notably, the presence of K suggests the potential of jarosite formation if bio-oxidation of sulfides is applied. It might cause the encapsulation of gold grains in the precipitates (Asamoah, 2021). Therefore, in the present work, the sulfide decomposition was carried out by ferric chloride leaching instead of bio-oxidation, as described below. The mineralogical compositions of the original DRGO consist of quartz (SiO_2), pyrite (FeS_2), magnesite ($MgCO_3$), chlorite (Mg, Fe, Mn, Ni)$_{6-x-yy}\square_x O_{10}(OH)_8$), muscovite ($KAl_2(AlSi_3O_{10})(OH)_2$), albite ($NaAlSi_3O_8$), and dolomite ($CaMg(CO_3)_2$), confirmed by X-ray diffraction (XRD, Rigaku, Ultima IV) with Cu Kα (40 kV, 40 mA). The particle size distribution of the original DRGO was determined by a laser scattering particle size distribution analyzer (HORIBA, Partica LA-950, Kyoto, Japan) showing that two peaks dominated around 10 μm and 60 μm, in which the former was predominant.

The graphitic degree of carbonaceous matters in the original DRGO from Syama mine and the other two DRGOs was evaluated by Raman spectroscopy (Thermo, DXR Smart Raman, Waltham, Massachusetts, USA, Fig. S1). In a range of 1200–1800 cm^{-1}, there are the characteristic peaks of graphitic carbon (G-band) at 1550–1650 cm^{-1} and defected

Table 1
Elemental compositions for solid residues after each pretreatment, determined by XRF.

Samples		Elemental compositions and their relative intensities (RI) normalized for Si contents																
		C	O	Na	Mg	Al	Si	P	S	K	Ca	Ti	Fe	Ni	Cu	Zn	As	others
DRGO	%(w/w)	6.83	41.75	1.00	1.67	7.45	15.69	0.07	6.13	1.98	3.11	0.55	13.38	0.03	0.10	0.08	0.08	0.38
	RI	0.435	2.661	0.064	0.106	0.475	1.000	0.004	0.391	0.126	0.198	0.035	0.853	0.002	0.006	0.005	0.005	–
DW	%(w/w)	6.09	39.49	1.16	0.83	8.37	18.28	0.03	8.35	2.43	0.24	0.56	13.80	0.05	0.10	0.10	0.10	0.32
	RI	0.333	2.160	0.063	0.045	0.458	1.000	0.002	0.457	0.133	0.013	0.030	0.755	0.003	0.006	0.005	0.005	–
DF	%(w/w)	8.38	40.98	1.34	0.38	8.28	19.24	0.01	7.18	2.56	0.03	0.57	9.99	0.03	0.07	0.06	0.06	0.98
	RI	0.436	2.130	0.069	0.020	0.430	1.000	0.001	0.373	0.133	0.001	0.030	0.519	0.001	0.004	0.003	0.003	–
DFW	%(w/w)	7.46	41.01	1.43	0.41	8.66	20.87	0.02	6.81	2.62	0.02	0.70	9.68	0.03	0.07	0.07	0.07	0.29
	RI	0.358	1.965	0.068	0.019	0.415	1.000	0.001	0.326	0.125	0.001	0.034	0.464	0.002	0.003	0.003	0.003	–
DFWC	%(w/w)	8.77	40.71	1.28	0.39	8.74	20.41	0.10	6.76	2.69	0.03	0.66	9.21	0.02	0.08	0.06	0.06	0.31
	RI	0.430	1.995	0.063	0.019	0.428	1.000	0.005	0.331	0.132	0.001	0.032	0.452	0.001	0.004	0.003	0.003	–
DFWY	%(w/w)	7.38	41.10	1.35	0.39	8.83	20.40	0.01	7.03	2.63	0.02	0.73	9.81	0.03	0.08	0.06	0.06	0.30
	RI	0.362	2.014	0.066	0.019	0.433	1.000	0.001	0.344	0.129	0.001	0.036	0.481	0.001	0.004	0.003	0.003	–
DFWCW	%(w/w)	7.99	41.85	1.41	0.44	8.83	20.79	0.02	6.00	2.66	0.03	0.72	9.07	0.03	0.09	0.06	0.06	0.17
	RI	0.385	2.013	0.068	0.021	0.425	1.000	0.001	0.289	0.128	0.002	0.034	0.436	0.002	0.004	0.003	0.003	–
DFWYW	%(w/w)	7.55	41.85	1.53	0.37	9.18	20.93	0.01	5.61	2.74	0.03	0.73	9.20	0.03	0.07	0.05	0.05	0.25
	RI	0.361	2.000	0.073	0.018	0.439	1.000	0.001	0.268	0.131	0.002	0.035	0.440	0.001	0.003	0.002	0.002	–

n.d.: not detected.

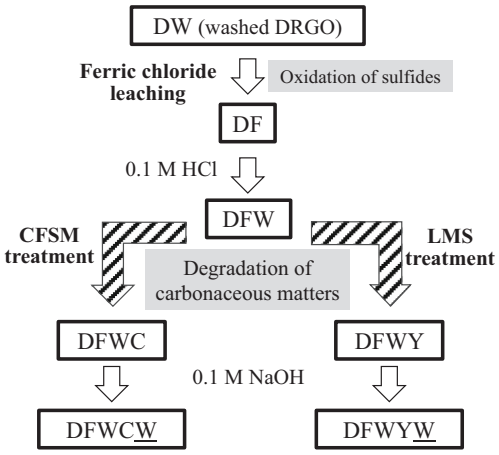

Fig. 2. Sequential pretreatment of DRGO including laccase-mediator system treatment. D: DRGO (double refractory gold ore), F: ferric chloride leaching with 0.5 M $FeCl_3$, W: washing with 0.1 M HCl, C: CFSM (cell free spent medium) treatment with *P. chrysosporium*, Y: LMS (laccase-mediated system) treatment with laccase Y-120, W: washing with 0.1 M NaOH. (For interpretation of the references to color in this figure legend, the reader is referred to the web version of this article.)

carbon (D-band) at 1300–1400 cm^{-1} (Liu et al., 2013; Lucchese et al., 2010). The graphitic degree was evaluated by the relative intensity of I_D/I_G using peak intensities of D-band and G-band, indicating that the smaller I_D/I_G values are the higher graphitic degrees, that is, the higher adsorption capacities of $Au(CN)_2^-$ (Zhang et al., 2012). The present DRGO from Syama mine was the more refractory and challenging to recover gold due to the higher value of I_D/I_G compared with the other two DRGOs (Amanya et al., 2017; Ofori-Sarpong and Osseo-Asare, 2013).

Based on the above, outline of the sequential pretreatments was designed in the present study as depicted in Fig. 2, where acid washing, ferric chloride leaching, enzyme treatment by LMS compared with CFSM, and then alkaline washing were arranged in the order. The details are described as follows.

2.2. Sample preparation, ferric chloride leaching and HCl washing

The DRGO used in this work is a flotation concentrates, so the original DRGO was firstly washed with pure ethanol (99%), 1 M HNO_3, and ultrapure water to remove the flotation reagents and soluble compounds (Mendoza et al., 2021b). The solid residue after washing was dried overnight in a freeze dryer and named DW and provided as the starting material for the following process.

In order to decompose sulfides for the liberation of gold grains, chemical leaching of DW with $FeCl_3$ was applied instead of bio-oxidation. A 40.00 g sample of DW was suspended in 800 mL of 0.5 M $FeCl_3$ at pH 1.0 adjusted with 1 M HCl in 2 L flasks. These flasks were shaken at 70 °C and 150 rpm for 24 h covered with a silicon cap to prevent water evaporation. At time intervals, the pH (TOA-DKK, GST-5841C, Tokyo, Japan) and the ORP vs the standard hydrogen electrode (SHE) using a reference electrode (TOA-DKK, PST—5821C, Tokyo, Japan) were monitored. The dissolved Fe^{2+} and Fe^{3+} concentrations were determined by the 1, 10-phenanthroline method.

Next, DF (Fig. 2) was washed with acid to decrease physically adsorbed Fe^{3+} ions on the surfaces. A 60.00 g sample of DF was suspended in 600 mL of 0.1 M HCl in 2 L flasks. These flasks were shaken at 25 °C and 150 rpm for 26 h. Then, the solid residues were washed with ultrapure water by centrifugation for 5 min at 25 °C and 10,000 rpm, and the process was repeated to reach a suitable pH (around pH 4) for the subsequent enzymatic reaction. Finally, the solid residue was named DFW.

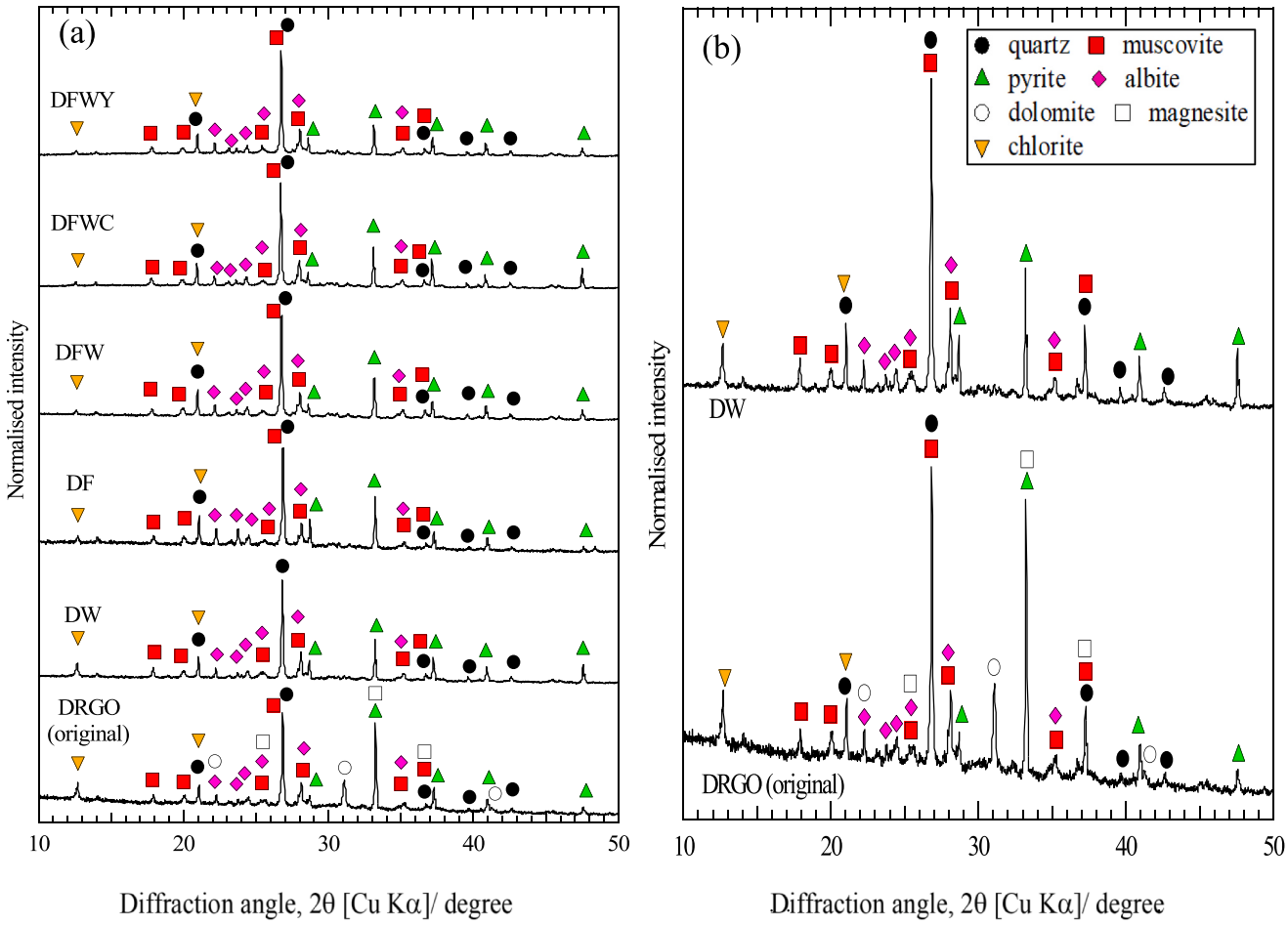

Fig. 3. XRD patterns for (a) solid residues after each pretreatment, and (b) the original DRGO and DW after expanded y-axis. Symbols: ●, quartz (PDF 00-033-1161); ▲, pyrite (PDF 00-042-1340); ○, dolomite (PDF 00–036-0426); ▼, chlorite (PDF 01-072-1234); ■, muscovite (PDF 01-072-0496); ◆, albite (PDF 01-071-6218); □, magnesite (PDF 01–071-6264).

2.3. Degradation of carbonaceous matter

2.3.1. Cell-free spent medium (CFSM) treatment

The LMS was compared with the conventional CFSM treatment; CFSM was obtained from the culture of *P. chrysosporium* in 2 L flasks containing 500 mL of the medium (Table S2) adjusted to pH 4 with 1 M NaOH. After 3 day-cultivation at 37 °C and 80 rpm, the CFSM was collected by filtration through Φ 0.22 μm Stericup® to remove any biomass like the fungal tissues. The enzyme activities of LiP and MnP in the CFSM were determined 20.6 ± 1.2 and 1.1 ± 0.2 U/L by spectrophotometry using veratryl alcohol and Mn^{2+} as substrates, respectively (Konadu et al., 2019b).

A 25.00 g sample of DFW was added to 500 mL of CFSM in the sterilized 2 L flasks and the mixture was shaken at 30 °C and 125 rpm. After 3 days, the solids were collected by centrifugation at 25 °C and 10,000 rpm for 5 min and resuspended in a fresh CFSM obtained from the continuous cultivation of *P. chrysosporium*. The 3 day-treatment was repeated 6 times, and the solid residues were named DFWC after 18 days. Therefore, the total enzyme activity of LiP and MnP was 130.2 U/L in CFSM treatment.

2.3.2. Laccase-mediator system (LMS) treatment

The purified Lcc (Y-120) derived from *Trametes* sp. was provided by courtesy of Amano Enzyme Inc. (Nagoya, Japan). A 25.00 g sample of DFW was suspended in the mixture of 498 mL of 0.1 M acetate buffer (CH_3COOH/CH_3COONa) at pH 4.5 and 1 mL of 1 M 1-hydroxybenzotriazole hydrate (HBT) dissolved in 99% ethanol in 2 L flasks. Separately 125 mg of purified laccase was dissolved in 1 mL of buffer, which was added to the above flask. These flasks were shaken at 30 °C and 125 rpm for 7 days. The initial enzyme activity of laccase (Y-120) was determined to be 118.7 ± 6.4 U/L, using 2,2′-azino-bis-(3-ethylbenzothiazoline-6-sulfonic acid) (ABTS) as a substrate with the molar absorption coefficient (ε) of 36,000 L mol^{-1} cm^{-1} at 420 nm (Baltierra-Trejo et al., 2015; Longe et al., 2018). These solid residues were collected and named DFWY. While established as a mediator as well as ABTS (Bourbonnais et al., 1997), 1-hydroxybenzotriazole (HBT) is well known to mediate the oxidation of lignin by laccase. There are also some reports to show the effect of HBT as a mediator for laccase-catalyzed reactions: degradation of lignin (Senthilvelan et al., 2017), oxidation of hydrocarbon (Cantarella et al., 2003) and degradation of non-phenolic lignin (Srebotnik and Hammel, 2000).

Furthermore, an additional treatment decreasing Lcc and HBT by half was conducted properly scrutinize and compare the LMS and CFSM treatments. The DFW residue was treated under the same conditions as LMS treatment, except for reducing Lcc (62.5 mg) and HBT concentration (1 mM) to half, where the initial Lcc activity was determined to be 65.6 ± 1.7 U/L. These solid residues were collected and named DFWY-half and provided to determine the gold recovery.

2.4. NaOH washing

The solid residues after both enzymatic treatments were washed with

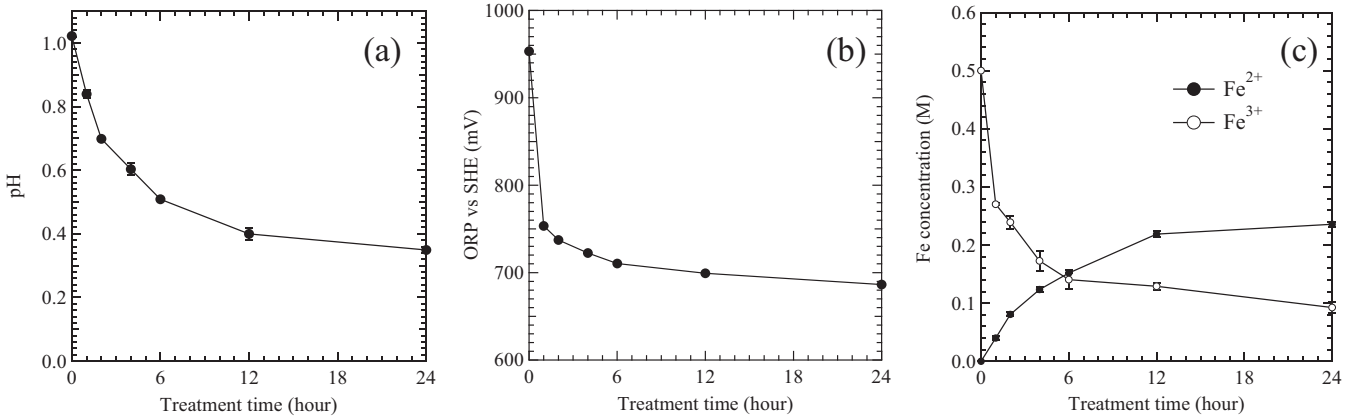

Fig. 4. Changes in (a) pH and (b) ORP (vs SHE), and (c) concentrations of Fe^{3+} and Fe^{2+} during chemical oxidation by 0.5 M $FeCl_3$.

0.1 M NaOH to remove the remaining degraded intermediates on the surfaces. A 5.00 g sample of each of DFWC and DFWY were separately added to 300 mL flasks containing 106.25 mL of 0.1 M NaOH. These flasks were shaken at 25 °C and 150 rpm for 24 h. The obtained solutions were supplied for three-dimensional (3D) fluorescence spectrometry (JASCO, FP-6600DS, Hachioji, Japan) to characterize the solubilized CM like humic substances. The solid residues were named DFWCW (from DFWC) and DFWYW (from DFWY).

2.5. Characterization for each solid residue

After each pretreatment described in Fig. 2, the elemental and mineralogical compositions were determined in the same manner as for the original DRGO. The chemical changes were also examined by using thermogravimetry differential thermal analysis (TG-DTA, Bruker, 2000SA, Billerica, Massachusetts) using α-Al_2O_3 as a reference, at 100 mL/min airflow and 5 °C/min heating rate. The graphitic degrees of CM were evaluated by Raman spectroscopy in the same manner as in the original DRGOs. The particle size distributions of the solid residues after each pretreatment were also determined in the same manner as for the original DRGO to observe the formation and decomposition of agglomerates.

2.6. Gold recovery

The gold extraction was performed by cyanidation of each solid residue. A 0.200 g sample of each solid was suspended in 4 mL of 2.5 mM KCN adjusted to pH 12 with 1 M KOH in 50 mL flasks. These flasks were shaken at room temperature and 134 rpm for 24 h. The pregnant leach solutions were supplied to determine the dissolved Au concentration (A) by inductively coupled plasma optical emission spectrometry (ICP-OES, Perkin Elmer Optima 8300, Waltham, Massachusetts, USA). The solid (leach) residues were also provided for subsequent acid digestion as described below.

First, 0.100 g of each solid residue was roasted at 800 °C for 4 h. Then, each roasted residue was added to the mixed concentrated acids, containing 3 mL HF (48%), 3 mL HNO_3 (60%), and 9 mL HCl (36%) in a Teflon vessel. The mixture was left overnight and then heated at 150 °C for 2 h in a Teflon/metal double jacket vessel. After confirming the complete dissolution of solid, the obtained liquid was provided to determine the concentration of Au dissolved from residue (B) by inductively coupled plasma mass spectrometry (ICP-MS, Agilent 7500c, Santa Clara, California, USA). Gold recovery was calculated by Eq. (1).

$$\text{Gold recovery}\ (\%) = (\mathrm{A})/((\mathrm{A}) + (\mathrm{B})) \times 100 \quad (1)$$

Since MLA results showed 5.86% of gold grains are enclosed in the acid-insoluble silicate minerals (quartz, albite, muscovite, orthoclase, illite, almandine, rutile) in the present DRGO as mentioned above, the present sequential treatment can be evaluated by normalization of each gold recovery for the extractable maximum by excluding gold enclosed in acid-insoluble silicates (Terry, 1983).

$$\text{Normalized gold recovery}\ (\%) = (\mathrm{A})/(((\mathrm{A}) + (\mathrm{B})) \times 0.9414) \times 100 \quad (1\prime)$$

3. Results and discussion

3.1. Sample preparation, ferric chloride leaching and HCl washing

The XRD patterns for DW and the original DRGO (Fig. 3(b)) elucidated that the main phase of encapsulated gold grains should be pyrite in the present DRGO because arsenopyrite and other sulfides were under the detection limit. In a process from DRGO to DW by washing with 1 M HNO_3, dolomite and magnesite were mostly dissolved (West and McBride, 2005). This was also supported by decrease in the relative intensities (RI) of C, O, Mg, and Ca contents obtained by XRF (Table 1, from DRGO to DW). The RI for each element is expressed as the elemental content (% *w*/w) normalized for Si content (% w/w), assuming that silicon is not dissolved from solid phase in each reaction. Considering the dissolution of carbonates (inorganic carbon), CM remaining in DW might have been mostly elemental and/or organic carbon both of which had a high preg-robbing capacity. Furthermore, since DW still contained 4.2 wt% of such carbon (Table S1), enzymatic degradation of CM is necessary for the present DRGO.

During ferric chloride leaching, the pH gradually decreased from 1 to 0.35 within 24 h (Fig. 4(a)), and the ORP rapidly decreased from 950 mV to 750 mV within 1 h and after that approached to the equilibrium (Fig. 4(b)). The Fe^{3+} concentration decreased from 0.5 M to 0.092 M within 24 h, and Fe^{2+} concentration increased to more than 0.23 M (Fig. 4(c)). Based on XRD (Fig. 3) and XRF (Table 1), the dissolved Fe species are mainly derived from pyrite in ferric chloride leaching, as shown in Eq. (2) under an acidic condition (Sasaki et al., 1995a; Bonnissel-Gissinger et al., 1998).

$$FeS_2 + 14Fe^{3+} + 8H_2O \rightarrow 15Fe^{2+} + 2SO_4^{2-} + 16H^+ \quad (2)$$

The reaction reached equilibrium within 24 h. The changes in XRD patterns of the solid residue from DW to DF showed a slight decrease in the relative peak intensities of pyrite (Fig. 3(a)). Dissolution of pyrite was also supported by the decrease in RI of Fe and S determined by XRF (Table 1). Additionally, no formation of jarosite was confirmed in XRD for DF.

Relative peak intensities of pyrite slightly decreased from DF to DFW in XRD (Fig. 3(a)), and RI of Fe and S contents in XRF (Table 1) decreased. This implies that 0.1 M HCl washing further dissolved pyrite and decreased the physically adsorbed Fe^{3+} ions on the surfaces, which

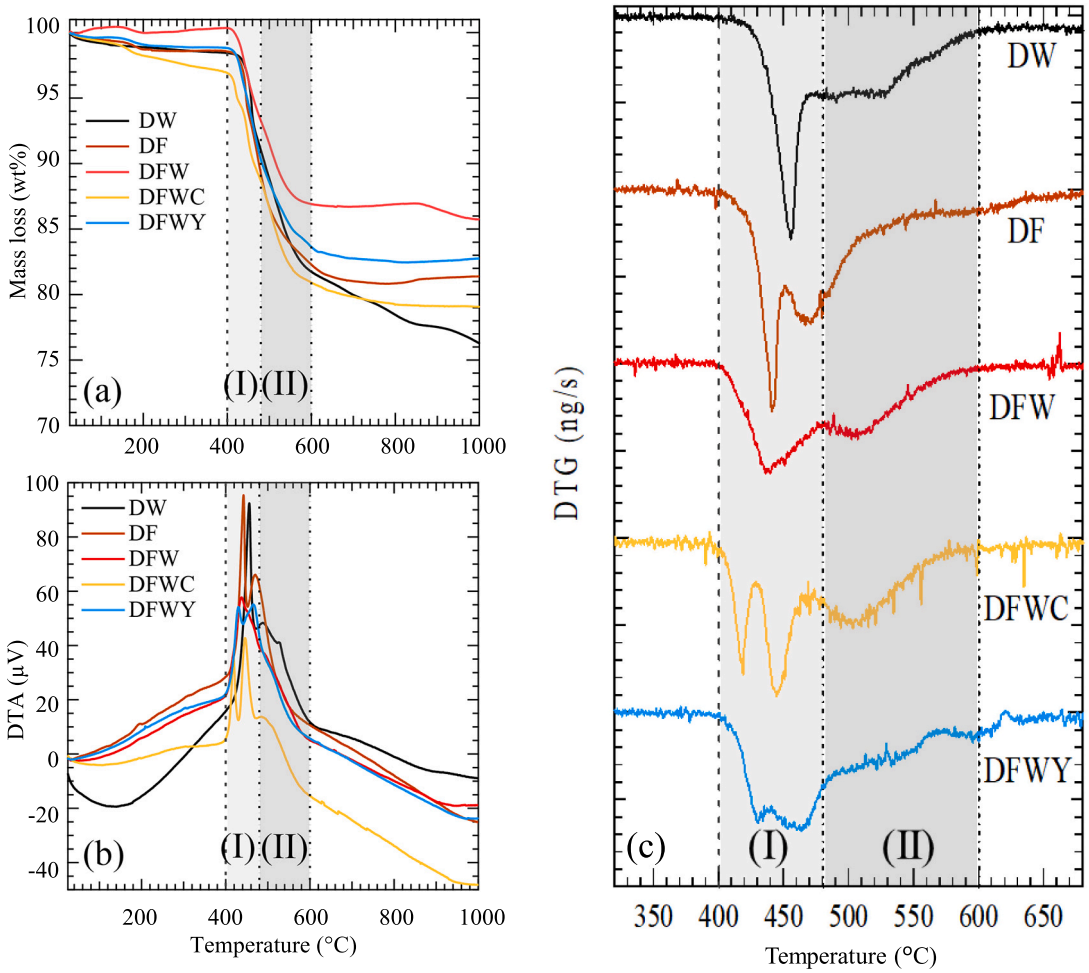

Fig. 5. Thermogravimetric analysis (TG-DTA) for solid residues after each pretreatment shown in Fig. 3, (a) mass loss (%), (b) DTA (μV), (c) DTG (ng/s).

is also supported by the results of TG-DTA analysis discussed below. In addition, XRD patterns also show a decrease in the relative peak intensity of chlorite due to the dissolution by 0.1 M HCl from DW to DF and from DF to DFW (Terry, 1983).

3.2. Degradation of carbonaceous matter

The TG-DTA result for each solid residue is shown in Fig. 5. Two primary ranges of weight loss were observed in DTG: (I) 400–480 °C for thermal decomposition of sulfides and (II) 480–600 °C for thermal decomposition of carbonaceous matter (Konadu et al., 2019a).

After ferric chloride leaching, the dominant DTG peak position was shifted from 455 °C for DW to 441 °C for DF (Fig. 5(c)). Then 0.1 M HCl washing broadened the DTG peak around 439 °C in DFW, keeping the peak position. This suggests sulfide bonds might be slightly cleaved by ferric chloride leaching and weakly bound sulfides might have been partially dissolved in 0.1 M HCl although the slight changes were only observed in XRD (Fig. 3(a)). Two enzymatic reactions differently revealed the effect on sulfide decomposition, not only the decomposition of carbonaceous matter. The DFWC showed two distinctive DTG peaks at 445 and 419 °C, while DFWY possesses a DTG peak at 434 °C and a broad DTG peak around 463 °C. The CFSM treatment partially damaged sulfides to more weakly bound sulfides because a new DTG peak appeared at 419 °C. The standard redox potentials for LiP, MnP, and Lcc are reported to be 1200–1500 mV, 1100 mV, and 960 mV, and LMS includes HBT as a mediator (Fakoussa and Hofrichter, 1999). They are high enough to attack the exposed pyrite, which has the standard redox potential of 270–340 mV (Sasaki et al., 1995b).

After CM degradation, the mass loss of DFWC (7.77% *w*/w) and DFWY (6.68% w/w) was smaller than DW (9.28% w/w) in the temperature range of 480–600 °C (Fig. 5(a)), suggesting that CM was degraded by each enzymatic treatment. Enzymes themselves consist of proteins, which should be decomposed at temperatures below 120 °C (Ku et al., 2009). However, it is notable that the mass loss might include the additional organic matter derived from biomolecules in CFSM. This would be one of the reasons why the mass loss at 480–600 °C was larger in DFWC than in DFWY. In addition, the DTG curves for DFWC and DFWY in a region of 480–600 °C show that the peak intensities more significantly decreased in DFWY than DFWC from DW. This implies that less CM remained in DFWY than DFWC, and LMS treatment was more efficient to degrade and solubilize the carbonaceous matter than CFSM treatment.

From an aspect of chemical bonding characteristics in CM, the changes in the graphitic degrees of CM were observed by Raman spectroscopy for the original DRGO, DFW, DFWC, and DFWY along with the values of I_D/I_G in Fig. 6. CM in DFWC showed a smaller value of I_D/I_G (1.02) than DFW (1.16), indicating that a part of defective carbon (D-band) might have been degraded and dissolved into the solution during CFSM treatment. On the other hand, CM in DFWY revealed a larger value of I_D/I_G (1.20) than DFW (1.16), implying that not only defective carbon (D-band) was degraded and dissolved but also a part of graphitic carbon (G-band) might have been converted into defective carbon (D-band) during LMS treatment. The differences in trend suggest that LMS treatment has degraded CM more effectively than CFSM treatment

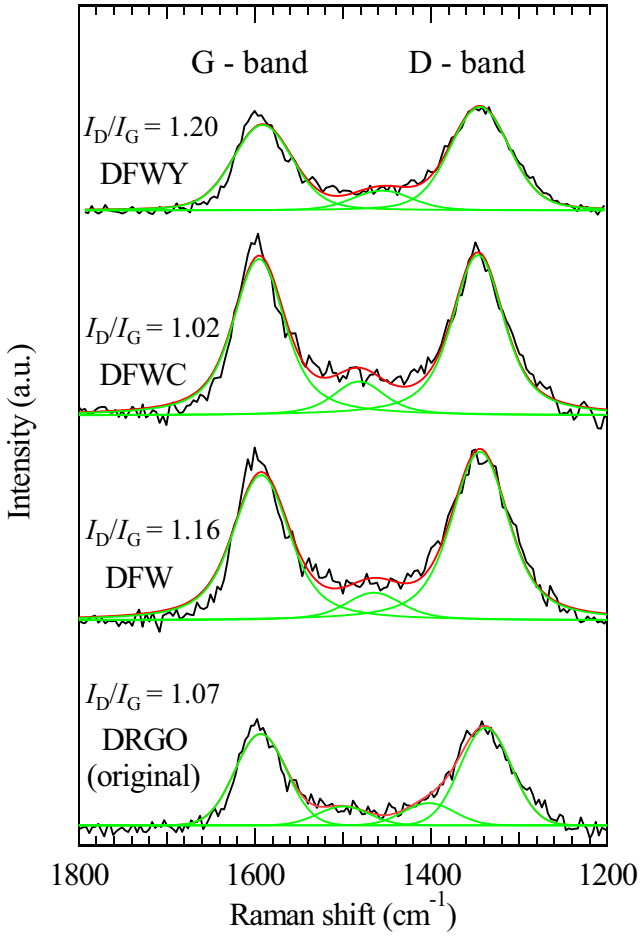

Fig. 6. Changes in Raman spectra for solid residues before and after enzymatic degradations of carbonaceous matter in DRGO in a region from 1200 cm^{-1} to 1800 cm^{-1} with relative intensities of I_D/I_G.

because graphitic carbon is more refractory and the main cause to adsorb $Au(CN)_2^-$ than defective carbon. This interpretation is also consistent with the observation in DTG (Fig. 5(c)).

Furthermore, 0.1 M NaOH washed solution of DFWC and DFWY were supplied to collect 3D fluorescence spectra, which give the characteristic information to humic-like substances. As shown in Fig. 7(a), (b), the peak positions are obviously different between the two, that is, they were located at E_m 510–520 nm and E_x 450 nm for the washed leachate from DFWC (Fig. 7(a)), and at E_m 400 nm and E_x 325 nm for the washed leachate from DFWY (Fig. 7(b)). According to the previous study (Gao et al., 2017), these peaks were ascribed to be humic-like substances with high molecular weight (E_m 500–525 nm, E_x 400–425 nm) and with lower molecular weight (E_m 400–450 nm, E_x 325–350 nm). Humic-like substances are known to have a wide range of molecular weights of 2000–10^6 Da (Perminova et al., 2003). In the present procedure, acid-insoluble fractions of carbonaceous matters were transferred into the enzymatic reactions because DFW was already gone through 0.1 M HCl washing. Since fulvic acid should be dissolved in all pH (Gaffney et al., 1996) and they would not be categorized into fulvic acid, it is reasonable to observe the 3D fluorescence peaks assigned to humic-like substances (Gao et al., 2017). The difference of the peak positions in 3D fluorescence spectra for two leachates strongly suggests CM degradation has been more advanced in LMS than CFSM treatment. The advantage of LMS to degrade CM into the lower molecular weight of humic-like substances might be derived from a function of HBT as a mediator. Separately, it was also confirmed that the peak at E_m 400–450 nm, E_x 325–350 nm was not derived from the HBT molecule. Based on the above, the mechanisms of CM degradation are completely different between CFSM treatment and LMS treatment, and this was also supported by the results of TG-DTA and Raman spectra. As mentioned above, TG-DTA results indicated carbonaceous matter was degraded more significantly in LMS than in CFSM, and Raman spectra suggested graphitic carbon was degraded into defective carbon as well as defective carbon in LMS treatment. As shown in Fig. 7 (inset), there is a clear contrast in the color of two leachates: dark brown color of the leachate after CFSM treatment seems to include higher concentrations of total organic carbon, in good agreement with the above interpretation.

Moreover, LMS treatment has several advantages over CFSM treatment in terms of experimental handling, higher stability of enzyme activity, a shorter reaction time, and no need to preculture the fungus. Depending on the initial condition of a white-rot fungus and its culture condition, the reproducibility of the initial enzymatic activity is much detrimentally affected in CFSM than in LMS treatment.

3.3. Gold recovery

Gold recovery of each solid residue resulted as summarized along with the procedures of sequential pretreatment in Fig. 8. Firstly, DW as the starting material had the lowest gold recovery (41.5 ± 0.3%), due to the encapsulation of gold grains in sulfides and adsorption of $Au(CN)_2^-$ on the originally existing CM.

Ferric chloride leaching and washing with 0.1 M HCl and ultrapure water could have increased gold recovery to 48.7 ± 10.9% for DF and

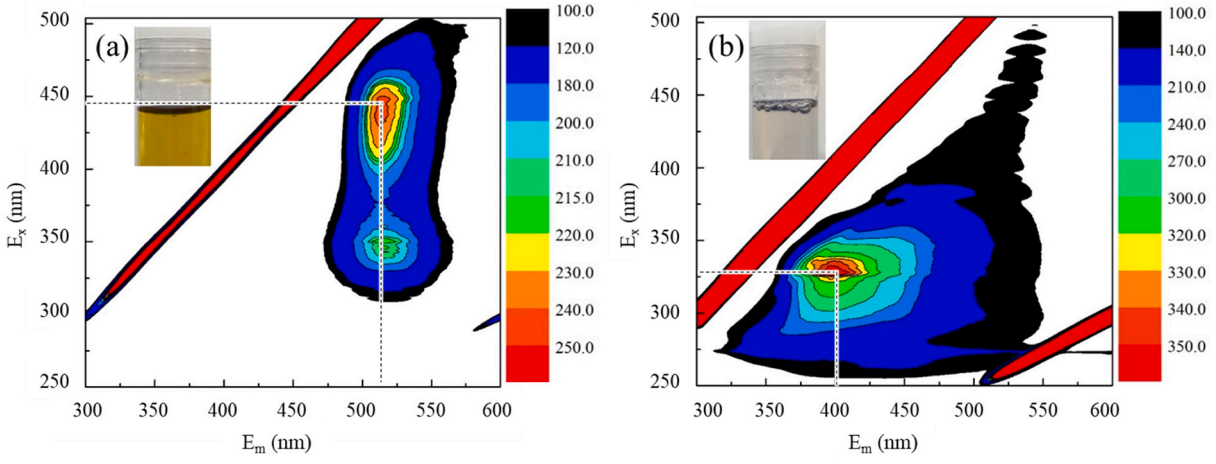

Fig. 7. Three-dimensional fluorescence spectra with the photographs of liquid residues after washing of (a) DFWC and (b) DFWY with 0.1 M NaOH.

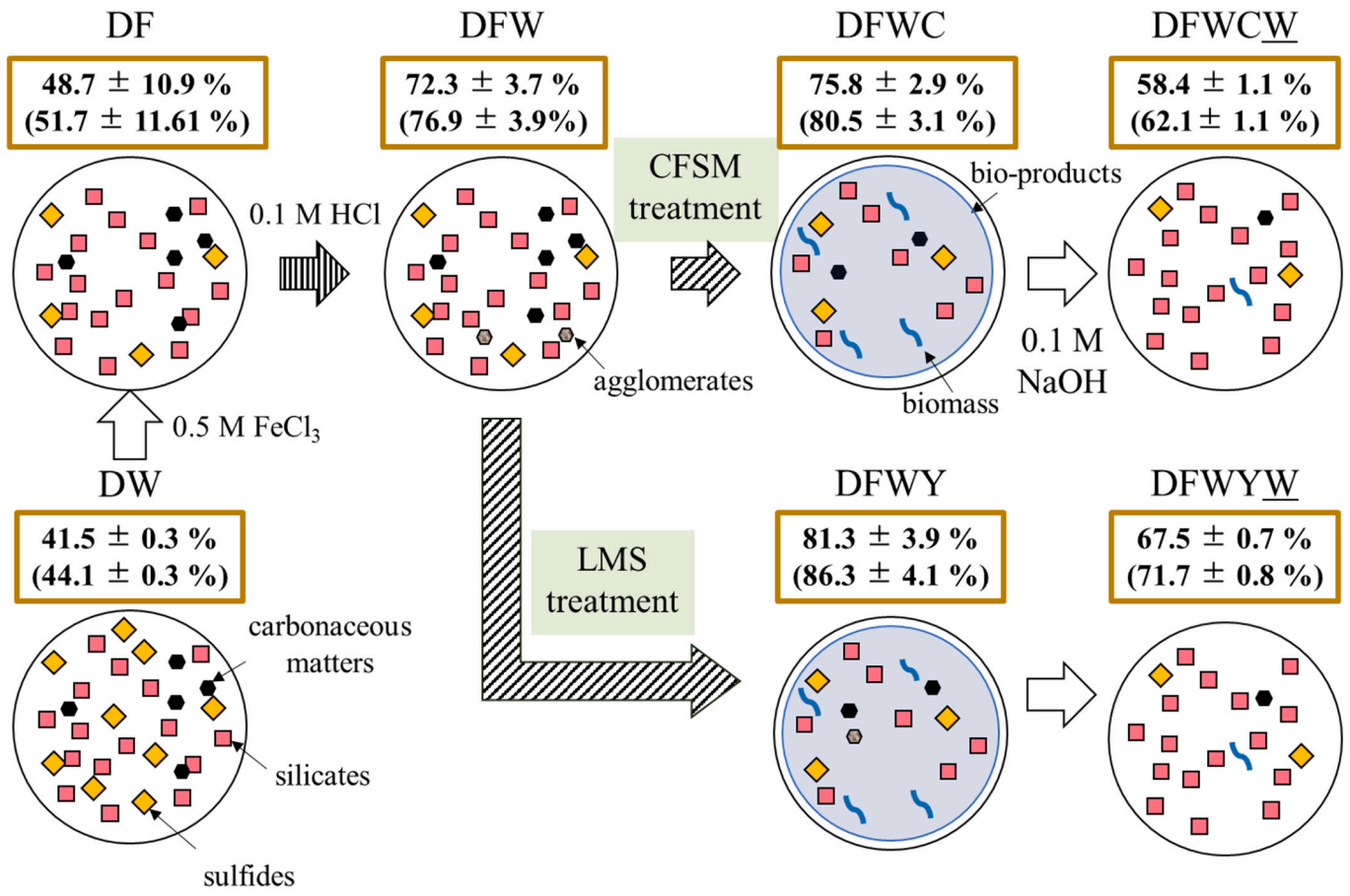

Fig. 8. Gold recoveries (%, $n = 2$) from the solid residues in the present sequential pretreatments of DRGO. Numbers in brackets indicate the normalized gold recovery after excluding the enclosed Au in silicates (5.86%) of the original ore. D: DRGO (double refractory gold ore), F: ferric chloride leaching with 0.5 M Fe^{3+}. Symbols: W: washing with 0.1 M HCl, C: CFSM (cell-free spent medium) treatment with *P. chrysosporium*, Y: LMS (laccase-mediator system) treatment with Y-120 (laccase), W: washing with 0.1 M NaOH. (For interpretation of the references to color in this figure legend, the reader is referred to the web version of this article.)

72.3 ± 3.7% for DFW. The reason for the lower gold recovery in DF than DFW, despite the liberation of some Au(0) grains by ferric chloride leaching, could be mainly attributed to residual Fe^{3+} and H^+ adsorbed on the ore surface after ferric chloride leaching. Residual Fe^{3+} ions might have consumed cyanide and the remaining H^+ lowered the pH during cyanidation, both of which might have diminished the recovery of gold. Because when the pH decreased below 10.5 during cyanidation, a fraction of cyanide (CN^-) was lost in the aqueous phase with the gasification to HCN, which is the hazardous species (Perry et al., 1999). On the other hand, gold recovery in DFW was much improved by decreasing the residual Fe^{3+} ions with 0.1 M HCl and the adsorbed H^+ with ultrapure water before cyanidation.

After CM degradation by CFSM treatment and LMS treatment, gold recovery was improved to 75.8 ± 2.9% for DFWC and 81.3 ± 3.9% for DFWY, respectively, suggesting that both treatments helped to reduce preg-robbing capacity. Also, the concentrations of dissolved gold during both CFSM and LMS treatment were small enough to ignore (< 0.12%). Although it was difficult to directly compare gold recovery with CFSM treatment due to the different substrates used for the enzyme activity assay in LMS treatment than in CFSM treatment, DFWY (after LMS treatment) showed the highest gold recovery of all samples. In an additional experiment, gold recovery of DFWY-half (the solid residue after LMS-half treatment) was 75.2 ± 3.1%. Even though the lower initial enzyme activity (65.6 ± 1.7 U/L), LMS treatment improved gold recovery from DFW.

Fig. S2 shows the relationship of gold recovery from gold ores against enzyme activity from LMS which was used for degradation of carbonaceous matter in gold ores, although these parameters are indirective. Considering all the gold recovery results and Fig. S2, LMS treatment is likely to show an advantage over CFSM treatment also from the efficiency standpoint of gold recovery.

The advantages of LMS in gold recovery were also reasoned by the interpretations obtained from TG-DTA (Fig. 5), Raman spectroscopy (Fig. 6), and 3D fluorescence spectrometry (Fig. 7). In particular, these characterizations have suggested that LMS treatment could be more efficient than CFSM treatment in the degradation of carbonaceous matter, even graphitic carbon. Additionally, LMS treatment showed various experimental superiorities compared to CFSM treatment as discussed above. Considering these above comparisons, LMS treatment could be a superior alternative process to CFSM treatment for CM degradation in DRGO.

After 0.1 M NaOH washing, gold recovery was 58.4 ± 1.1% for DFWCW and 67.5 ± 0.7% for DFWYW, both of which were lower than before washing. The decrease might be caused by the following reasons. In these sequences, 0.5 M ferric chloride leaching was introduced for the dissolution of sulfides. Under strongly alkaline conditions, the residual Fe^{3+} ions might have easily caused the precipitation of hydroxide and/or oxyhydroxide. Then, these precipitates could encapsulate tiny Au(0) grains and/or consume cyanide during cyanidation, resulting in the gold recovery loss similar to the case of jarosite. Thus, 0.1 M NaOH washing after CM degradation may strongly diminish the recovering gold in the case of such ores bearing relatively large amounts of Fe^{3+} ions.

The maximum gold recovery was 81.3 ± 3.9% for DFWY, which is correspondent to 86.3 ± 4.1% after normalization for the extractable maximum based on Eq. (1). All gold recoveries before and after normalization were summarized in Fig. 8. These values of the gold

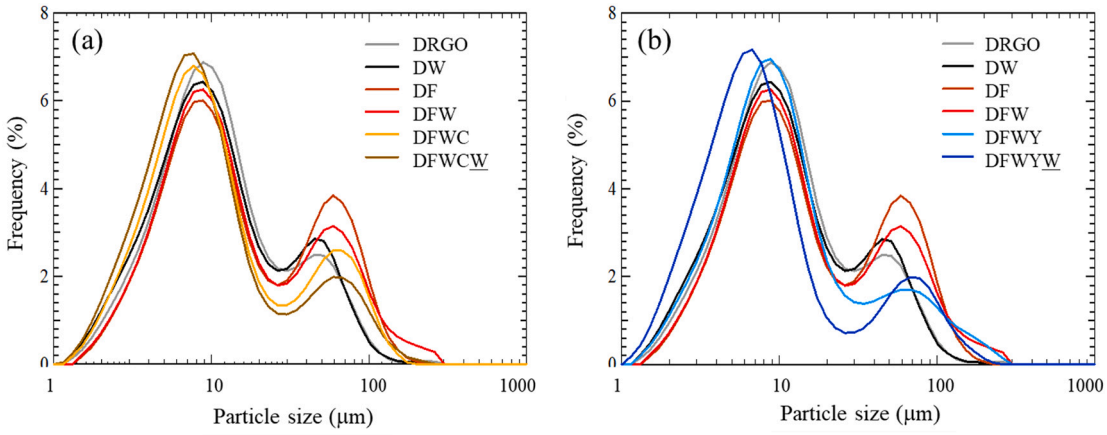

Fig. 9. Particle size distributions for solid residues after each pretreatment shown in Fig. 2 ($n = 3$). (a) DRGO → DW → DF → DFW → DFWC → DFWCW, (b) DRGO → DW → DF → DFW → DFWY → DFWYW.

recovery can be further improved using stronger condition of cyanidation optimizing the several parameters including temperature, concentration of CN^-, and extraction time. For the perfect extraction of gold, further stronger conditions of ferric chloride leaching (temperature, pressure) and finer grinding of the original ore can be considered to dissolve sulfide minerals further.

3.4. Changes in the particle size distributions and evaluation of 0.1 M HCl washing

The particle size distribution was analyzed for each solid residue for further understanding the reaction in each step (Fig. 9). In all samples, there are two large peaks around 4–20 μm with the peak top of 8–10 μm and around 20–100 μm with the peak top of 50–70 μm. Compared to DW, there are trends that the relative frequencies of the 1st peak (< 20 μm) slightly increased, and the relative frequencies of the 2nd peak (around 20–100 μm) decreased in DFWC and DFWY. Considering these trends, the 1st peaks (< 20 μm) could be mainly derived from CM and silicate minerals and 2nd peaks (20–100 μm) could include the dominant fractions of sulfide. The attribution of particle sizes is also consistent with the peaks of silicate and CM (Konadu et al., 2019b) and the peaks of sulfide (Mendoza et al., 2021b; Zhou and Cabri, 2004) described in the previous studies.

In the process from DW to DF, the frequency of particle sizes around 20–40 μm decreased by the dissolution of pyrite, while the frequency of particle sizes around 40–100 μm increased. In addition, from DF to DFW, the frequency peak of the particle sizes around 40–100 μm has shifted to 100–300 μm. These changes might be due to agglomeration among silicates and/or CM mediated through residual Fe^{3+} ions working as a bridge. Namely, ferric chloride leaching enhanced agglomerations, and 0.1 M HCl washing facilitated further agglomeration. Decreases in frequencies of the 1st peak (< 20 μm) mainly derived from silicates and CM particles, which should not be dissolved by ferric chloride leaching and HCl washing, support this interpretation. On the other hand, C-Si-Al agglomerates (described in Section 1) were not newly observed in DFWC and DFWY. Finally, the effect of 0.1 M NaOH washing on the decomposition of agglomerates can be seen in both DFWCW (40–60 μm) and DFWYW (100–300 μm).

Comprehensively, the effects of the washing with 0.1 M HCl and ultrapure water can be summarized as follows. Washing with 0.1 M HCl and ultrapure water has contributed to the slight dissolution of pyrite and the decreases in Fe^{3+} and H^+ as discussed in Section 3.1 and 3.3. Although new agglomerations that might interfere with recovering gold in DFW were produced, the improvement in gold recovery from DF to DFW supported the effectiveness of washing with 0.1 M HCl and ultrapure water. Further detailed mechanism and effects of HCl washing will be discussed elsewhere.

4. Conclusions

In the sequential pretreatment of double refractory gold ore (DRGO) from Syama mine, laccase-mediator system (LMS) was applied for the first time to the degradation of carbonaceous matter in the real DRGO to improve the gold recovery.

Ferric chloride leaching was adopted to dissolve sulfides to avoid the formation of jarosite. Subsequent washing with 0.1 M HCl and ultrapure water decreased the remaining Fe^{3+} and H^+, resulting in the improved gold recovery to 72.3 ± 3.7% from 41.5 ± 0.3% in the starting material.

Then, LMS treatment was applied for CM degradation, in which laccase was combined with 1-hydroxybenzotriazole (HBT) as a mediator. The LMS had advantages over cell-free spent medium (CFSM) including LiP and MnP from *Phanerochaete chrysosporium*, that is, the stability, availability, and reaction time. The characterization of degraded and remaining carbonaceous matter revealed that LMS was capable of more efficient and advanced CM degradation than CFSM, including the degradation of graphitic carbon. This led the maximum gold recovery of 81.3 ± 3.9% after LMS treatment, which was greater than after CFSM treatment. This value corresponds to 86.3 ± 4.1% after normalization for the extractable maximum gold excluding enclosed gold in acid-insoluble silicates, suggesting the LMS treatment contributed to improve the gold recovery with 9.4%, greater than CFSM treatment with 3.6%.

Thus, LMS treatment could be considered as a superior alternative process for the degradation of carbonaceous matter for DRGO. Finally, the most effective sequential pretreatment can be proposed for the present DRGO in the order of ferric chloride leaching, washing with 0.1 M HCl and ultrapure water, and laccase-mediator system treatment. In this way, the sequential process should be designed to customize, depending on the chemical and mineralogical compositions of ores.

Declaration of Competing Interest

None.

Acknowledgments

The authors appreciate the financial supports of JSPS KAKENHI JP19KK0135, and JSPS International Exchange Programs JPJSBP120196505, JPJSBP120219929, JPJSCCB20200003, which were provided to KS. Laccase (Y-120) was supplied by courtesy of Amano Enzyme Co. Ltd. DRGO from Syama mines, Mali was provided by courtesy of Prof. Jacques Eksteen at Curtin University.

Appendix A. Supplementary data

Supplementary data to this article can be found online at https://doi.org/10.1016/j.hydromet.2022.105894.

References

Abotsi, G.M.K., Osseo-Asare, K., 1986. Surface chemistry of carbonaceous gold ores I. characterization of the carbonaceous matter and adsorption behavior in aurocyanide solution. Int. J. Miner. Process. 18, 217–236. https://doi.org/10.1016/0301-7516(86)90019-0.

Amanya, F., Ofori-Sarpong, G., Anni, V., Amankwah, R.K., 2017. Preg-robbing of gold by carbonaceous materials encountered in gold processing. Ghana Min. J. 17, 50–55. https://doi.org/10.4314/gm.v17i2.7.

Anderson, C.G., 2016. Alkaline sulfide gold leaching kinetics. Miner. Eng. 92, 248–256. https://doi.org/10.1016/j.mineng.2016.01.009.

Asamoah, R.K., 2021. Specific refractory gold flotation and bio-oxidation products: research overview. Minerals. 11, 1–14. https://doi.org/10.3390/min11010093.

Baltierra-Trejo, E., Márquez-Benavides, L., Sánchez-Yáñez, J.M., 2015. Inconsistencies and ambiguities in calculating enzyme activity: the case of laccase. J. Microbiol. Methods 119, 126–131. https://doi.org/10.1016/j.mimet.2015.10.007.

Bas, A.D., Ghali, E., Choi, Y., 2017. A review on electrochemical dissolution and passivation of gold during cyanidation in presence of sulphides and oxides. Hydrometallurgy 172, 30–44. https://doi.org/10.1016/j.hydromet.2017.06.021.

Bonnissel-Gissinger, P., Alnot, M., Ehrhardt, J.J., Behra, P., 1998. Surface oxidation of pyrite as a function of pH. Environ. Sci. Technol. 32, 2839–2845. https://doi.org/10.1021/es980213c.

Bourbonnais, R., Paice, M.G., Freiermuth, B., Bodie, E., Borneman, S., 1997. Reactivities of various mediators and laccases with Kraft pulp and lignin model compounds. ASM Appl. Environ. Microbiol. 63, 4627–4632. https://doi.org/10.1128/aem.63.12.4627-4632.1997.

Cantarella, G., Galli, C., Gentili, P., 2003. Free radical versus electron-transfer routes of oxidation of hydrocarbons by laccase/mediator systems catalytic or stoichiometric procedures. J. Molecular Cat. B 22, 135–144. https://doi.org/10.1016/S1381-1177(03)00014-6.

Fakoussa, R.M., Hofrichter, M., 1999. Biotechnology and microbiology of coal degradation. Appl. Microbiol. Biotechnol. 41, 347–348. https://doi.org/10.1016/s0140-6701(00)94135-3.

Gaffney, J.S., Marley, N.A., Clark, S.B., 1996. Humic and fulvic acids and organic colloidal materials in the environment. ACS Symp. Ser. 651 https://doi.org/10.1021/bk-1996-0651.ch001.

Gao, J., Liang, C., Shen, G., Lv, J., Wu, H., 2017. Spectral characteristics of dissolved organic matter in various agricultural soils throughout China. Chemosphere 176, 108–116. https://doi.org/10.1016/j.chemosphere.2017.02.104.

Guzman, I., Thorpe, S.J., Papangelakis, V.G., 2018. Redox potential measurement during pressure oxidation (POX) of a refractory gold ore. Can. Metall. Q. 57, 382–389. https://doi.org/10.1080/00084433.2017.1386363.

Konadu, K.T., Sasaki, K., Kaneta, T., Ofori-Sarpong, G., Osseo-Asare, K., 2017. Bio-modification of carbonaceous matter in gold ores: model experiments using powdered activated carbon and cell-free spent medium of *Phanerochaete chrysosporium*. Hydrometallurgy 168, 76–83. https://doi.org/10.1016/j.hydromet.2016.08.003.

Konadu, K.T., Huddy, R.J., Harrison, S.T.L., Osseo-Asare, K., Sasaki, K., 2019a. Sequential pretreatment of double refractory gold ore (DRGO) with a thermophilic iron oxidizing archeaon and fungal crude enzymes. Miner. Eng. 138, 86–94. https://doi.org/10.1016/j.mineng.2019.04.043.

Konadu, K.T., Harrison, S.T.L., Osseo-Asare, K., Sasaki, K., 2019b. Transformation of the carbonaceous matter in double refractory gold ore by crude lignin peroxidase released from the white-rot fungus. Int. J. Biodeterior. Biodegrad. 143, 104735 https://doi.org/10.1016/j.ibiod.2019.104735.

Konadu, K.T., Mendoza, D.M., Huddy, R.J., Harrison, S.T.L., Kaneta, T., Sasaki, K., 2020. Biological pretreatment of carbonaceous matter in double refractory gold ores: a review and some future considerations. Hydrometallurgy 196, 105434. https://doi.org/10.1016/j.hydromet.2020.105434.

Ku, T., Lu, P., Chan, C., Wang, T., Lai, S., Lyu, P., Hsiao, N., 2009. Predicting melting temperature directly from protein sequences. Comput. Biol. Chem. 33, 445–450. https://doi.org/10.1016/j.compbiolchem.2009.10.002.

Liu, J., Li, Q., Zou, Y., Qian, Q., Jin, Y., Li, G., Jiang, K., Fan, S., 2013. The dependence of graphene Raman D-band on carrier density. Nano Lett. 13, 6170–6175. https://doi.org/10.1021/nl4035048.

Liu, Q., Yang, H.Y., Tong, L.L., Jin, Z.N., Sand, W., 2016. Fungal degradation of elemental carbon in carbonaceous gold ore. Hydrometallurgy 160, 90–97. https://doi.org/10.1016/j.hydromet.2015.12.012.

Longe, L.F., Couvreur, J., Leriche Grandchamp, M., Garnier, G., Allais, F., Saito, K., 2018. Importance of mediators for lignin degradation by fungal laccase. ACS Sustain. Chem. Eng. 6, 10097–10107. https://doi.org/10.1021/acssuschemeng.8b01426.

Lucchese, M.M., Stavale, F., Ferreira, E.H.M., Vilani, C., Moutinho, M.V.O., Capaz, R.B., Achete, C.A., Jorio, A., 2010. Quantifying ion-induced defects and Raman relaxation length in graphene. Carbon 4, 1592–1597. https://doi.org/10.1016/j.carbon.2009.12.057.

Mendoza, D.M., Ichinose, H., Konadu, K.T., Sasaki, K., 2021a. Degradation of powder activated carbon by laccase-mediator system: model experiments for the improvement of gold recovery from carbonaceous gold. J. Environ. Chem. Eng. 9, 106375 https://doi.org/10.1016/j.jece.2021.106375.

Mendoza, D.M., Konadu, K.T., Aoki, Y., Kameya, M., Sasaki, K., 2021b. Carbonaceous matter degradation by fungal enzyme treatment to improve ag recovery from an au-ag-bearing concentrate. Miner. Eng. 163, 106768 https://doi.org/10.1016/j.mineng.2020.106768.

Nanthakumar, B., Pickles, C.A., Kelebek, S., 2007. Microwave pretreatment of a double refractory gold ore. Miner. Eng. 20, 1109–1119. https://doi.org/10.1016/j.mineng.2007.04.003.

Norgate, T., Haque, N., 2012. Using life cycle assessment to evaluate some environmental impacts of gold production. J. Clean. Prod. 29–30, 53–63. https://doi.org/10.1016/j.jclepro.2012.01.042.

Ofori-Sarpong, G., Osseo-Asare, K., 2013. Preg-robbing of gold from cyanide and non-cyanide complexes: effect of fungi pretreatment of carbonaceous matter. Int. J. Miner. Process. 119, 27–33. https://doi.org/10.1016/j.minpro.2012.12.007.

Ofori-Sarpong, G., Tien, M., Osseo-Asare, K., 2010. Myco-hydrometallurgy: coal model for potential reduction of preg-robbing capacity of carbonaceous gold ores using the fungus, *Phanerochaete chrysosporium*. Hydrometallurgy 102, 66–72. https://doi.org/10.1016/j.hydromet.2010.02.007.

Owusu, C., Mensah, S., Ackah, K., Amankwah, R.K., 2021. Reducing preg-robbing in carbonaceous gold ores using passivative or blanking agents. Miner. Eng. 170, 106990 https://doi.org/10.1016/j.mineng.2021.106990.

Perminova, I.V., Frimmel, F.H., Kudryavtsev, A.V., Kulikova, N.A., Abbt-Braun, G., Hesse, S., Petrosyan, V.S., 2003. Molecular weight characteristics of humic substances from different environments as determined by size exclusion chromatography and their statistical evaluation. Environ. Sci. Technol. 37, 2477–2485. https://doi.org/10.1021/es0258069.

Perry, R., Browner, R.E., Dunne, R., Stoitis, N., 1999. Low pH cyanidation of gold. Miner. Eng. 12, 1431–1440. https://doi.org/10.1016/s0892-6875(99)00132-6.

Qin, H., Guo, X., Tian, Q., Yu, D., Zhang, L., 2021. Recovery of gold from sulfide refractory gold ore: oxidation roasting pretreatment and gold extraction. Miner. Eng. 164, 106822 https://doi.org/10.1016/j.mineng.2021.106822.

Sasaki, K., Tsunekawa, M., Ohtsuka, T., Konno, H., 1995a. Confirmation of a sulfur-rich layer on pyrite after oxidative dissolution by Fe(lll) ions around pH2. Geochim. Cosmochim. Acta 59, 3155–3158. https://doi.org/10.1016/0016-7037(95)00203-C.

Sasaki, K., Tsunekawa, M., Hasebe, K., Konno, H., 1995b. Effect of anionic ligands on the reactivity of pyrite with Fe(III) ions in acid solutions. Colloids Surf. A Physicochem. Eng. Asp. 101, 39–49. https://doi.org/10.1016/0927-7757(95)03142-Z.

Senthilvelan, T., Kanagaraj, J., Panda, R.C., 2017. Enhanced biodegradation of lignin by laccase through HOBT mediator: mechanistic studies supported by FTIR and GCMS studies. Environ. Process. https://doi.org/10.1007/s40710-017-0209-z.

Srebotnik, E., Hammel, K.E., 2000. Degradation of nonphenolic lignin by the laccase/1-hydroxybenzotriazole system. J. Biotechnol. 81, 179–188.

Suzuki, I., 2001. Microbial leaching of metals from sulfide minerals. Biotechnol. Adv. 19, 119–132. https://doi.org/10.1016/S0734-9750(01)00053-2.

Terry, B., 1983. The acid decomposition of silicate minerals part I. Reactivities and modes of dissolution of silicates. Hydrometallurgy 10, 135–150. https://doi.org/10.1016/0304-386X(83)90002-6.

Wang, G., Liu, X., Wu, Y., Zeng, T., Li, S., Liu, J., Liu, Y., Xie, S., 2020. Bio-oxidation of a high-sulfur refractory gold concentrate with a two-stage chemical-biological approach. Hydrometallurgy 19, 105421. https://doi.org/10.1016/j.hydromet.2020.105421.

West, T.O., McBride, A.C., 2005. The contribution of agricultural lime to carbon dioxide emissions in the United States: dissolution, transport, and net emissions. Agric. Ecosyst. Environ. 108 (2), 145–154.

Yang, H.Y., Liu, Q., Song, X.L., Dong, J.K., 2013. Research status of carbonaceous matter in carbonaceous gold ores and bio-oxidation pretreatment. Trans. Nonferrous Metals Soc. China 23, 3405–3411. https://doi.org/10.1016/S1003-6326(13)62881-2.

Zhang, C., Lu, G., Sun, Z., Yu, J., 2012. Catalytic graphitization of carbon/carbon composites by lanthanum oxide. J. Rare Earths 30, 128–132. https://doi.org/10.1016/S1002-0721(12)60008-8.

Zhou, J.Y., Cabri, L.J., 2004. Gold process mineralogy: objectives, techniques, and applications. JOM 56, 49–52. https://doi.org/10.1007/s11837-004-0093-7.